ORIGINAL PAPER



Modelling, manufacturing and testing of acoustic plate resonator liners

Vincent Radmann¹ · Moritz Neubauer² · Julia Genßler³ · Fleming Kohlenberg^{1,3} · Simon Jekosch¹

Received: 14 March 2025 / Revised: 27 May 2025 / Accepted: 3 June 2025 © The Author(s) 2025

Abstract

This paper presents the results of a study in which the concept of the plate resonator as an acoustic engine liner was thoroughly investigated from an acoustic and a manufacturing perspective. Since future jet engines will present new challenges such as low-frequency tonal noise, e.g. due to larger fans, new lining concepts need to be developed to solve these future noise problems. The plate resonator concept represents a possible alternative to conventional linings. Therefore, a semi-analytical model is used to carry out extensive parameter studies to better understand the fundamental operating mechanisms of plate resonators. A suitable plate material for the resonator is also derived from the parameter studies. Based on this, a plate resonator liner prototype is designed and additional investigations are carried out to determine the properties of the considered material. Afterwards, the design is manufactured in lightweight construction taking into account the engine-specific requirements. To verify this concept, measurements are carried out in an aeroacoustic test rig investigating two plate resonator liners. Thereby, the effects of pre-tension applied to the plates and grazing flow are analysed. The aim of realising low-frequency attenuation under the condition of limited installation space is successfully achieved by the plate resonator concept. In addition, the capability of using the semi-analytical model for specific design purposes is proven. The feasibility of implementing this concept in a jet engine nacelle is also investigated by considering a lightweight manufacturing process. The results of this work provide a solid base for new lining concepts and contribute to the goal of making future air traffic much quieter.

 $\textbf{Keywords} \ \ Acoustic \ damping \cdot Acoustic \ liner \cdot Manufacturing \cdot Novel \ liner \ concepts \cdot Aircraft \ noise \cdot Plate \ resonator$

1 Introduction

The most effective way to attenuate sound is to prevent its generation at the source. However, this is often not feasible and, therefore, silencers are employed where sound propagation in flow ducts needs to be attenuated. The nacelle of an aircraft engine can be considered a special type of flow duct,

Published online: 03 October 2025

- ¹ Institute of Fluid Dynamics and Engineering Acoustics, Technische Universität Berlin, Einsteinufer 25, 10587 Berlin, Germany
- Institute of Lightweight Engineering and Polymer Technology (ILK), Technische Universität Dresden, Holbeinstr. 3, 01307 Dresden, Germany
- ³ Institute of Propulsion Technology, Engine Acoustics, German Aerospace Center (DLR), Bismarckstr. 101, 10623 Berlin, Germany

with silencers typically located in the inlet and outlet. These silencers are known as liners and usually consist of honeycomb cells covered by a perforated face sheet, which forms an array of Helmholtz resonators. A Helmholtz resonator in turn consists of a cavity whose dimensions are small compared to the wavelength considered. This cavity is connected to the environment by a small hole in the face sheet [1]. The attenuation of Helmholtz resonators is comparatively narrow-band.

To increase fuel efficiency, aircraft engines are developed towards larger fans and bypass ratios. A larger fan with a higher bypass ratio can provide the same thrust at lower jet speeds and rotational frequencies. However, this leads to new acoustic challenges that the liners have to address. In detail, this means that a large slow-rotating fan will lead to low-frequency tonal noise, caused by a lower Blade-Pass-Frequency [2]. Additionally, the overall noise spectrum is assumed to be more broadband than in current engines. However, larger fans will not lead to larger nacelles, so it can



be expected that less installation space is available for future liners. In summary, this means thinner liners are needed to achieve low-frequency and broadband attenuation, although these two requirements are often contradictory. Therefore, new advanced liner technologies are needed to address these challenges.

Because of their acoustic properties, plate resonators (PR) offer a concept for future liners to tackle all these problems. They consist of a thin flexible plate that covers a cavity completely [3]. Plate resonators effectively attenuate low-frequency noise [4]. Beyond their acoustic capabilities, plate resonators have certain advantages that make them a suitable application in jet engines. Unlike perforated structures, they are insensitive to contamination caused by particles carried by the flow. Furthermore, the smooth and closed surface also prevents particles from entering the cavity and offers only very low resistance to the grazing flow [5]. Due to these abilities, plate resonators are commonly used in ventilation and exhaust systems and are therefore suitable for application as aircraft engine liners, too [6].

To use plate resonators as liners effectively, suitable tools are required to design these silencers. First investigations to evaluate the applicability of plate resonators for jet engines date back to 1969 [7]. However, the so far most advanced model was introduced by Huang and Wang [3, 8]. This model has been studied in different ways considering the flexible structure as a membrane or a plate respectively and with different boundary conditions [9–11]. In a previous project by the authors, the plate resonator model was examined in a two-dimensional, dimensionless framework, i.e. without physical units [5]. To improve the model's accuracy and investigate realisable applications, it was extended in a three-dimensional form and with physical units. In addition, this semi-analytical approach is capable to take grazing flow into account and was validated by Finite Element Method (FEM) and measurements in an acoustic flow duct [12].

The semi-analytical model was employed in [13] to conduct preliminary parameter studies and examine the impact of individual material and geometry parameters on transmission loss. Furthermore, a theoretical manufacturing concept for the production of curved plate resonator liners was developed, but it was not put into practice or subject to experimental evaluation.

In this study, the semi-analytical model is used to extend parameter investigations to obtain a more precise understanding of the impact of individual parameters on the attenuation effect of plate resonators. Based on these and using the approach given in [14] a suitable material for jet engine application is identified. In addition, material-specific investigations are carried out to determine the properties of the considered plate material. Following the selection and investigation of a suitable plate material, the semi-analytical model is applied to design a liner prototype. Then, a lightweight manufacturing approach

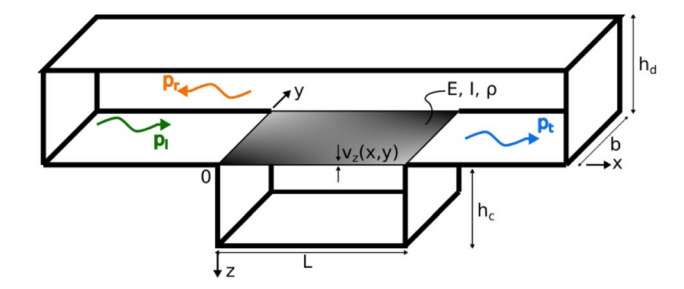


Fig. 1 Sketch of a simple plate resonator

is investigated and a flat liner prototype is build. Compared to [13], a different manufacturing concept is used, which could actually be implemented as part of this study. The scattering coefficients of the manufactured prototype are then measured in an acoustic flow duct test rig, considering the effect of grazing flow. Finally, these results are compared to those calculated by the semi-analytical model and by finite-element-method (FEM).

Compared to previous considerations in [13], this study provides a more detailed view on the impact of the individual material parameters, the properties of the considered plate material and the specific design of a plate resonator liner using the semi-analytical model. Furthermore, it shows how a flat plate resonator liner consisting of several cavities is manufactured and how the experimentally determined scattering coefficients compare to the semi-analytical model and the FEM for this liner prototype.

2 Modelling

The following section provides an introduction to the semianalytical model of a plate resonator. The schematic structure of a simple PR is shown in Fig. 1, which serves as the baseline for modelling. A part of the hard duct wall is replaced by a thin flexible plate, which is simply supported on all four edges. If a sound wave is travelling along the duct $(p_{\rm in})$ and hits the PR, the plate starts to oscillate. This causes an interaction with the closed cavity beneath the plate. Due to this, one part of the incident sound energy is reflected back in the direction of the source (p_r) . Another amount of the incoming sound energy is dissipated by intrinsic material damping within the plate. The superposition of the remaining portion of the incident sound combined with the sound emitted by the plate in the same direction leads to the overall transmitted sound (p_t) , which carries less energy than the incident one. In a former project, a semi-analytical approach was used to describe this behaviour of the plate resonator [5]. The model behind has been originally introduced by Huang and Wang [3, 15]. In this work, this approach is used in a 3D and dimensional way to model this principle as



realistic as possible. In the following, a brief outline of the model is shown. For more details refer to [12].

The starting point of the modelling is the bending differential equation of a thin flexible plate:

$$B\nabla^4 v_z + m'' \frac{\partial^2}{\partial t^2} v_z = -\frac{\partial}{\partial t} (p_+ - p_-). \tag{1}$$

Where v_z is the velocity of the plate and the parameter to be determined in (1). Furthermore, the left-hand side contains the bending stiffness B and the mass per unit area m'' of the plate. On the right-hand side the pressure difference above (p_+) and below (p_-) the plate represent the source mechanism of the differential equation. To solve this equation, a modal approach is applied in the first step. Therefore, the plate velocity can be described as a sum of mode functions φ_{jk} with the corresponding amplitude v_{jk} where the indices describe the mode order. The type of the mode functions is determined by the boundary conditions of the plate. Due to the simply supported boundary conditions and in accordance with [16] the following applies for the plate velocity:

$$v_{z} = \sum_{i,k} v_{jk} \varphi_{jk} \tag{2}$$

$$\varphi_{jk} = \sin\left(\frac{j\pi x}{L}\right) \sin\left(\frac{k\pi y}{b}\right).$$
(3)

The modal approach of the plate velocity is inserted into Eq. (1) and afterwards a Galerkin Method is applied in order to solve the bending differential equation. Therefore, Eq. (1) is multiplied by an arbitrary base function φ_{lm} which is chosen here corresponding to the base function to exploit the resulting simplifications. Afterwards, both sides of the differential equation are integrated over the area of the plate. Thus, on the left-hand side of Eq. (1) orthogonality relations between mode and base functions can be exploited to simplify the result. On the right-hand side, the pressure difference can be expressed in terms of the plate velocity's modal amplitude and a so-called impedance matrix. This allows to build a linear system of equations in which v_{jk} can be isolated and calculated:

$$\left(L_{jkjk} + Z_{c,jklm} + Z_{d,jklm}\right)v_{jk} = -I_{lm}.\tag{4}$$

Eq. (4) contains the matrix L_{jkjk} which contains the material properties of the flexible plate. Furthermore, the matrices $Z_{c,jklm}$ and $Z_{d,jklm}$ describe the sound field inside the cavity and the sound field above the plate which is radiated into the duct. $Z_{c,jklm}$ based on an room acoustic approach to describe the sound field inside the cavity. To describe the sound field emitted by the plate into the duct, which is described by $Z_{d,jklm}$, the starting point is the radiation pressure of a flush to the wall point source. To describe the total radiation pressure

of the plate, a distributed source is formed by integrating many point sources over the entire plate surface. A possible grazing flow in the duct is also considered by incorporating the Mach number in $Z_{d,jklm}$. However, due to brevity, the formulas are not presented here. A detailed description of this can be found in [15]. On the right-hand side, the inhomogeneity describes the incident sound considering only plane waves. Thus, the only unknown in Eq. (4) is the amplitude of the plate velocity, which allows the equation to be solved.

The calculated modal amplitude of the plate v_{jk} can now be used to determine the sound radiated by the plate in both directions of the duct. Thus, the scattering coefficients of the plate resonator can be calculated to quantify the liner's performance. So, the transmission coefficient T is defined as the ratio of the transmitted and incident sound power and the following relation applies in this case:

$$T = \left| \frac{p_t}{p_{in}} \right|^2 = \left| \lim_{x \to \infty} \frac{p_{+rad}|_{s,t=0}}{p_{in}} + 1 \right|^2.$$
 (5)

In Eq. (5) the sound pressure which is radiated by the plate is evaluated for the fundamental mode (s, t = 0) and along the direction of the incident sound $(x \to \infty)$. A similar approach can be used to calculate the reflection coefficient R. Therefore, p_{+rad} is evaluated at $x \to -\infty$, excluding the incident sound from the superposition. The dissipation coefficient of the plate resonator can then be calculated using T and R under consideration of the grazing flow:

$$\Delta = 1 - (T + \frac{1 - M}{1 + M}R). \tag{6}$$

Furthermore, the transmission coefficient can be used to calculate the transmission loss TL of the plate resonator using the following formula:

$$TL = -10\log_{10}(T). (7)$$

The validity of this approach has already been investigated and has been demonstrated in various publications [5, 12–14]. In the following, this model is also utilized in a two-dimensional form (see [5]), taken into account physical units. Furthermore, the implementation of the semi-analytical model was published as an open-source Python package [17].

3 Parameter studies and material selection

A suitable geometry and plate material are essential for the successful application of the plate resonator concept as a jet engine liner. The first step is to examine the effect of input parameters on plate resonator attenuation. In this section, several parameter studies are performed to gain a deeper



understanding of the plate resonator's behavior. These parameter studies utilize the two-dimensional approach of the semi-analytical model to minimize computational effort. Given the objective of identifying general trends resulting from input parameters, the two-dimensional approach is a suitable choice.

The input parameters and the parameter intervals of the plate resonator model can be seen in Tab. 1. The dimensions of the duct (duct height and cavity depth) are based on the test rig which is used for the liner prototype measurements later (see Sect. 5). According to a theoretical installation space for a liner the intervals for cavity length and height are chosen. For plate material value ranges are selected corresponding to the material classes of polymers and thermoplastic elastomers following the Ashby diagram [18]. These material classes are chosen because they can exhibit high intrinsic material damping, unlike metals. Only one parameter is varied according to the value range in Tab. 1, while the other parameters remain the design point values.

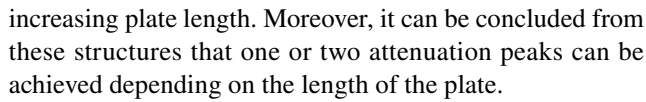
3.1 Results of the parameter studies

The variations of the geometry parameters can be seen in Fig. 2. On the x-axis the frequency is located and the varied parameter on the y-axis of the respective plot. The transmission loss (TL) is represented by the colour. The lighter the colour, the higher the transmission loss.

Fig. 2a shows the variation in plate length respectively in cavity length. It is particularly noteworthy that s-shaped structures occur in the transmission loss. These shapes are caused by the natural modes of the plate. The order of the natural modes depends on the frequency and length of the plate. The courses of the theoretical natural modes of the plate are also shown in Fig. 2a. Thus, it can be observed that the transmission loss asymptotically approaches the courses of the odd modes and reaches its maximum width when it intersects with the even modes. This causes jumps in the frequency of the transmission loss maximum with

Table 1 Input parameters for the semi-analytical model

Plate material	6 cm/[1 cm; 10 cm] 3 cm/[1 cm; 10 cm] 8 cm/-
cavity height h_c cavity width b (3D) cavity width b (2D) duct height h_d plate height h_p O.3	3 cm/[1 cm; 10 cm]
cavity width b (3D) cavity width b (2D) duct height h_d plate height h_p 0.3	
cavity width b (2D) duct height h_d plate height h_p 0.3	8 cm/-
duct height h_d plate height h_p 0.3 Plate material	
plate height h_p 0.3 Plate material	∞ /-
Plate material	6 cm/-
	$mm/[0.05\ mm;0.5\ mm]$
density ρ_n 110	
J P P	$00 \mathrm{kg/m^3/} [800 \mathrm{kg/m^3}]$
	$;2800 \mathrm{kg/m^3}]$
Young's modulus E	
loss factor η	1 GPa/[10 MPa; 10 GPa]



A similar pattern can also be seen considering the variation of the plate thickness, see Fig. 2c. However, there is a significant shift in the frequency of the s-shaped patterns. So, a thicker plate leads to a low-frequency attenuation and also one or two damping peaks can be achieved. Considering the cavity height, it can be seen clearly that a higher cavity leads to a lower-frequency transmission loss, see Fig. 2b. This relation is not linear but approaches a frequency of approx. 400Hz for increasing height. In addition, a second transmission loss peak appears for higher cavities.

Figure 3 shows the results of the transmission loss, regarding the variation of the plate material parameters. In Fig. 3a it can be seen, that the variation of Young's modulus leads to distinctive s-shaped patterns which are caused by the natural modes as well. Globally, there is a slight shift of the transmission loss to lower frequencies and the s-shaped patterns are drawn apart with an increasing Young's modulus. Again, this shows that the choice of the Young's modulus affects whether one or two transmission loss peaks are present.

In contrast, a higher loss factor leads to a more broadband but less strong transmission loss, as expected, see Fig. 3b. And a higher density of the plate material shifts the *TL* to lower frequencies, similar to the cavity height, see Fig. 3c.

3.2 Material selection

The studies of the geometric and material-specific parameters provide a fundamental understanding of how the plate resonator works but also serve as a basis for a meaningfull material selection. It can be seen that some parameters show clear trends while others develop s-shape structures. However, what has not yet been taken into account varying the material parameters is that the Young's modulus and the loss factor cannot be considered independently. Stiff materials such as metals usually don't have high material damping while polymers with high material damping usually are more flexible. Therefore, a functional relation between Young's modulus and loss factor has been used for the considered material class of the polymers and thermoplastic elastomers. For more details, please refer to [14]. This investigation finally leads to the decision for a thermoplastic polyurethane (TPU). The final simulation using the design point and the material properties of TPU, which can be found in Tab. 2 is shown in Fig. 4. In this case, the three-dimensional approach has been used to calculate the transmission loss.

Besides TPU, ethylen butylacrylat (EBA) emerged as a potentially suitable material for plate resonator liners. Both materials were subjected to material-specific tests to



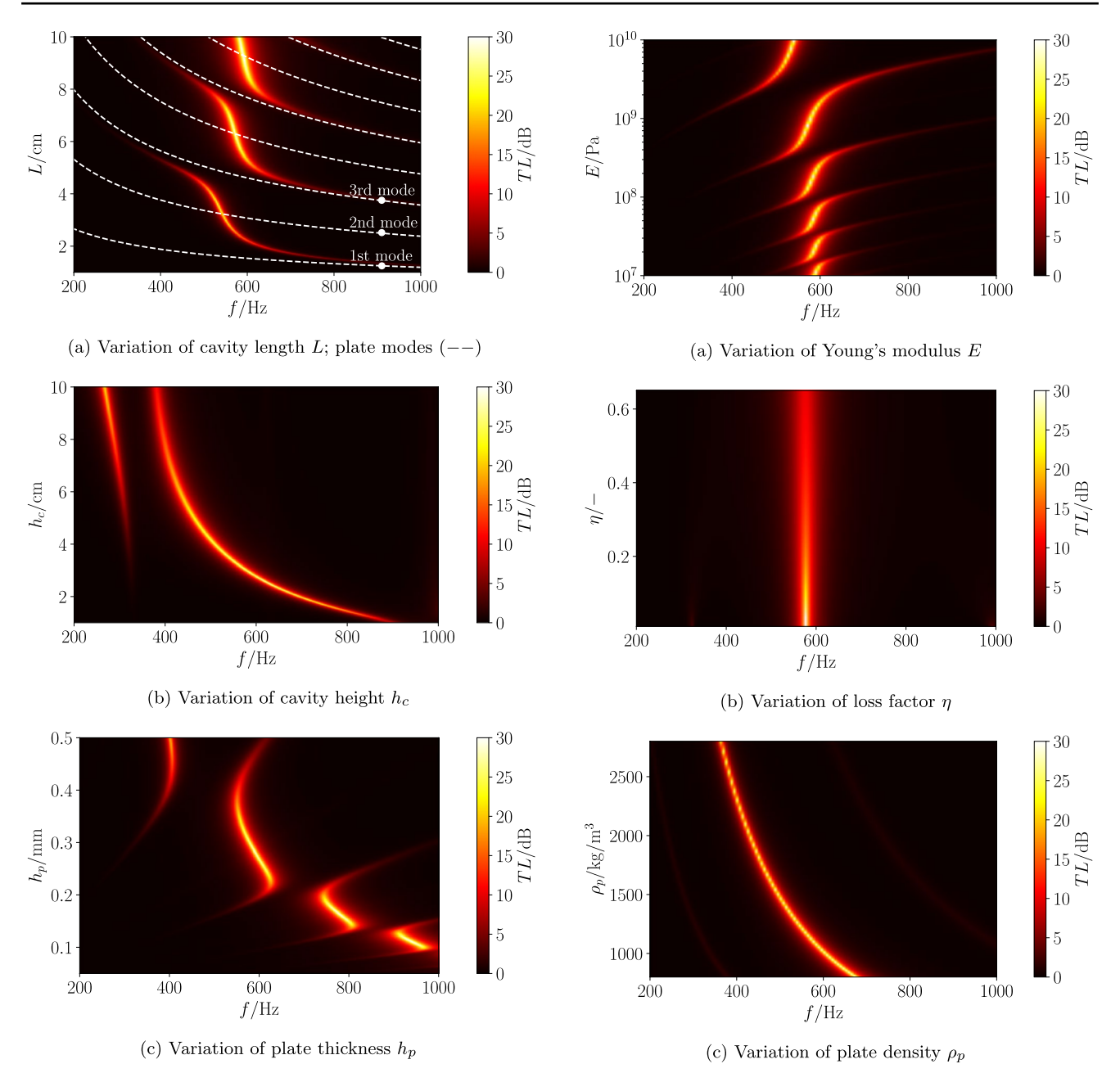


Fig. 2 Colour maps of the transmission loss (*TL*) of a single-chamber plate resonator under variation of different geometry parameters

Fig. 3 Colour maps of the transmission loss (TL) of a single-chamber plate resonator under variation of different material parameters

determine their suitability for use in jet engines. However, only TPU was used to fabricate a prototype liner.

3.3 Material investigations

In addition to the acoustic investigations, material-specific tests were conducted on the two materials under consideration. These tests were carried out in collaboration with Fraunhofer PYCO, who conducted various experiments to characterise the material properties, such as dynamic mechanical analysis (DMA). Furthermore, the impact of various engine-specific factors was also examined, including the effects of temperature fluctuations, UV radiation, exposure to water, jet fuel, hydraulic oil, and ethylene glycol, which is used as a de-icing agent. The samples were exposed to these conditions for 1000h each.

No noticeable increases in weight were observed due to exposure of water or ethylene glycol indicating that the materials are resistant to these influences. The residence in



jet fuel causes a slight increase of weight for TPU and a strong one for EBA. A similar trend was observed for EBA under the influence of hydraulic oil. TPU, however, showed signs of deterioration. Exposure to UV radiation did not lead to any visible changes in TPU while EBA showed signs of embrittlement.

These tests provided important insights into the usability of these materials for jet engine liners. Even if some criteria are to be assessed as problematic, others show that the considered material is well suited for the intended use. Therefore, it is conceivable that other plastic mixtures could be found that fulfil the engine-specific requirements even better without sacrificing the acoustic performance.

4 Liner prototype

The following section takes a closer look at the PR liner prototype. First, the requirements and design specifications are explained and afterwards the manufacturing of the PR liner is shown.

4.1 Requirements and design

Larger fans that can rotate at lower speeds and produce the same thrust are expected in future engines. This lower rotation speed leads to low-frequency tonal noise, which must be damped. Thus, the target frequency for the damping maximum was set at 650Hz. However, since the attenuation should be as broadband as possible, the transmission loss should be half as the maximum at 650Hz for a range ± 70 Hz. The liner should also be effective under grazing flow conditions. Therefore, this design should work at a M=0.2 with upstream sound propagation.

Apart from the acoustics, probably the most crucial criteria are the installation space and the weight of the liner. In accordance with current liner technology, a maximum installation height of 43mm is therefore specified. However, the entire length (22cm) and width (8cm) are determined by the test rig. It is also intended to divide the liner into several chambers

Table 2 Material properties of the TPU plate

Parameter	Value
TPU	
density ρ_p	1080kg/m ³
Young's modulus E	14MPa
loss factor η	0.1
plate height h_p	0.3mm

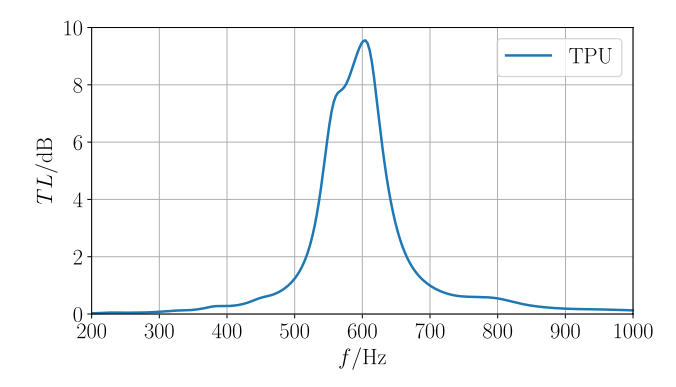


Fig. 4 Transmission loss of a plate resonator with a TPU-1170A plate; calculated with the three-dimensional approach; design point geometry

to exploit similarities to current liner concepts. Additionally, small holes to equalize static pressure differences are needed, as otherwise, the plates are likely to inflate under grazing flow.

With this requirements, additional calculations were carried out with the semi-analytical model to design a PR liner that fulfils the requirements as far as possible. The findings from the parameter studies were used to adjust the cavity geometries of the plate resonator liner. This adjustment was made to achieve the target frequency range using the TPU as the plate. The result was a 3x2 PR liner with the specifications in Tab. 3. The manufacturing of the PR line is described in the next section.

4.2 Manufacturing

The PR liner can be divided into the reinforced support and flexible plate section based on the applied materials. The selection process for the plate material has been thoroughly explained in section 3.2 and in [14]. The material used for the resonator body has a minor impact on the acoustic performance as long as it is sufficiently rigid to not enable any body vibrations. The primary functions are to provide the resonator cavity, ensure the structural integrity, and support load-bearing requirements. For the present investigation, a polyamide-6 organic sheet with 60% continuous glas fiber reinforcement (PA6-GF) was selected. The choice was based on the good availability of the semi-finished product in various wall thicknesses and surface dimensions, as well as its proven structural performance in comparable applications, such as the Helmholtz resonator liner, which has already been confirmed through simulations [13]. In addition to the low specific density, the similar melting temperature ranges offer further advantages, particularly for joining processes. The selected semi-finished product (1mm thickness) was precisely and efficiently cut into the required components (stringers, film carrier, and bottom plate) using a waterjet process. The finished individual components are shown in Fig. 5.



The design of the planar test sample was implemented using a simple plug-in principle by introducing grooves into the stringers as well as the film carrier and bottom plates. The plug-in assembly process of the liner is shown in Fig. 6(a). To ensure the bond of the components and to prevent the transmission of airborne sound between the resonator cavities, the joints between the components are sealed with the two-component adhesive (DP490, 3MTMScotch-WeldTM). In preliminary studies, the feasibility of using ultrasonic welding to join the film to the support structure was evaluated, aiming to leverage the benefits of matching material groups and melting temperatures. Since achieving consistent film pre-tension during the process proved challenging, the film was alternatively applied to the carrier using a double-sided polyurethanebased adhesive film of the type 4032, 3MTM(see Fig. 6(b)). This configuration allows for easy replacement of the film material and systematic variation of pre-tensioning conditions. Ideally, the TPU film should be applied without pretensioning. However, as this was not possible without the formation of wrinkles, slight pre-tension was required to smooth them out. Therefore, the film is pre-tensioned inplane by attaching fastening clamps with equipped weights to the edges of the film, using a custom-designed apparatus to enable a force-controlled tensioning process (see Fig. 6(c)). The film is stretched over a PTFE support plate to minimise friction. After the pre-tensioning process, the resonator body with the film carrier is positioned on the support plate and bonded to the film with light pressure. Finally, a cannula is inserted into the outer wall of one cavity to ensure proper static pressure equalisation during acoustic performance testing in the duct under grazing flow conditions. To ensure this pressure equalisation between all cavities, the walls between them are drilled by a 0.6mm diameter hole. Since the film was applied to the resonator using an adhesive film and can be removed without damaging the resonator, the same resonator body could be reused to investigate the influence of films with different pre-tension values. The finished planar PR liner sample is shown in Fig. 6(d). Since the actual goal of an assembly without any pre-tensioning at all was not possible, this circumstance was used to investigate the effect of different pre-tensions on the attenuation effect of the PR liner. Within the scope of this investigation, two different pre-tensions of the film were analysed. For the first liner, a minimal pre-tension of 1N in both planar directions was applied. This was necessary in order to smooth out the film for a proper application, although this liner was basically to be manufactured without pre-tensioning. For the second liner, a pre-tension of 10N was exerted using the tensioning device.

5 Measurements and finite element method

In the following section, the setups for the measurements and the numerical simulations by a finite element method are introduced. The results of both methods are then shown and compared with those of the semi-analytical model.

5.1 Experimental setup

The PR liner prototypes were experimentally investigated at the DUCT-R (duct acoustic test rig with a rectangular cross section). The test rig is part of the measurement facilities of the German Aerospace Center (DLR) in Berlin. A schematic illustration of the structure of the duct is shown in Fig. 7. The DUCT-R is divided into three sections. In sections 1 and 2, five 1/4''G.R.A.S. 40BP-S1 microphones are flush mounted to the walls to reduce interaction with the grazing flow. The microphone sections are separated by the test section where the liner sample can be placed. At each end of the duct, a speaker of the type BMS 4599HE (A and B) is placed to excite the sound field inside the duct. In addition, there are two non-reflecting terminations at the ends of the duct. Thus, the end-reflections are reduced to 15% or below for frequencies above 160Hz. Consequently, a frequency of 160Hz can be regarded as a cut-on frequency, above which the impact of end-reflections on measurement outcomes can be considered insignificant. The cross section of the duct is 60mm by 80mm which leads to a cut-on frequency of 2142Hz of the first higher mode. Furthermore, a radial compressor is attached to the duct to create a grazing flow with a center line Mach number up to 0.3.

To determine the scattering coefficients of the considered liner, the sound field inside the duct is excited either by speaker A or B using single tones. Both are able to produce sound pressure levels up to 130dB which is necessary to reach a good signal to noise ratio during measurements with flow. Due to the five microphones on each side of the test section, the sound field inside the duct is decomposed into upstream and downstream travelling sound waves. Thus, the decomposed sound field can be used to determine the scattering coefficients (transmission T, reflection R and dissipation Δ) upstream and downstream of the test section. The test rig has a low error of less than 3% for the determined dissipation and has already been used in many other

Table 3 Geometrical specifications of the PR liner prototype

Parameter	Value
cavity length L	67mm
cavity width b	39mm
cavity height h_c	25mm



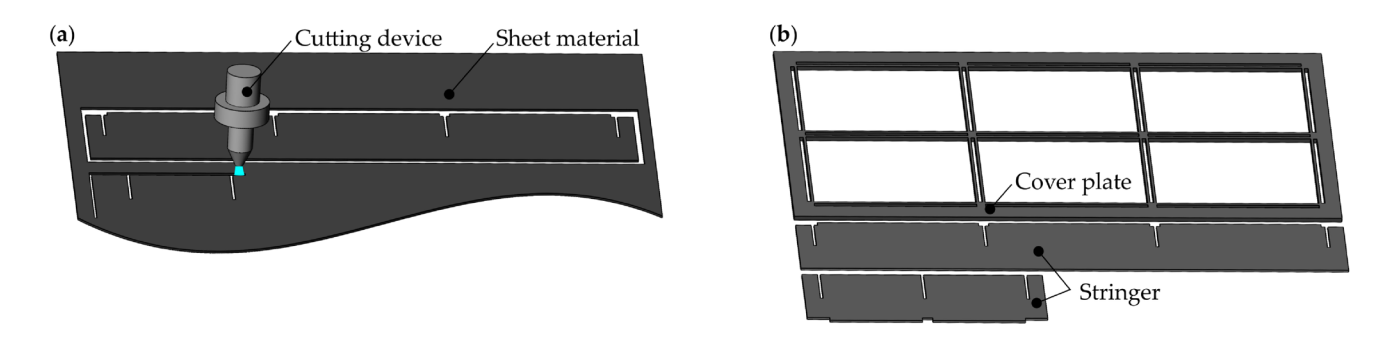


Fig. 5 Water jet cutting process of the individual components of the planar liner samples

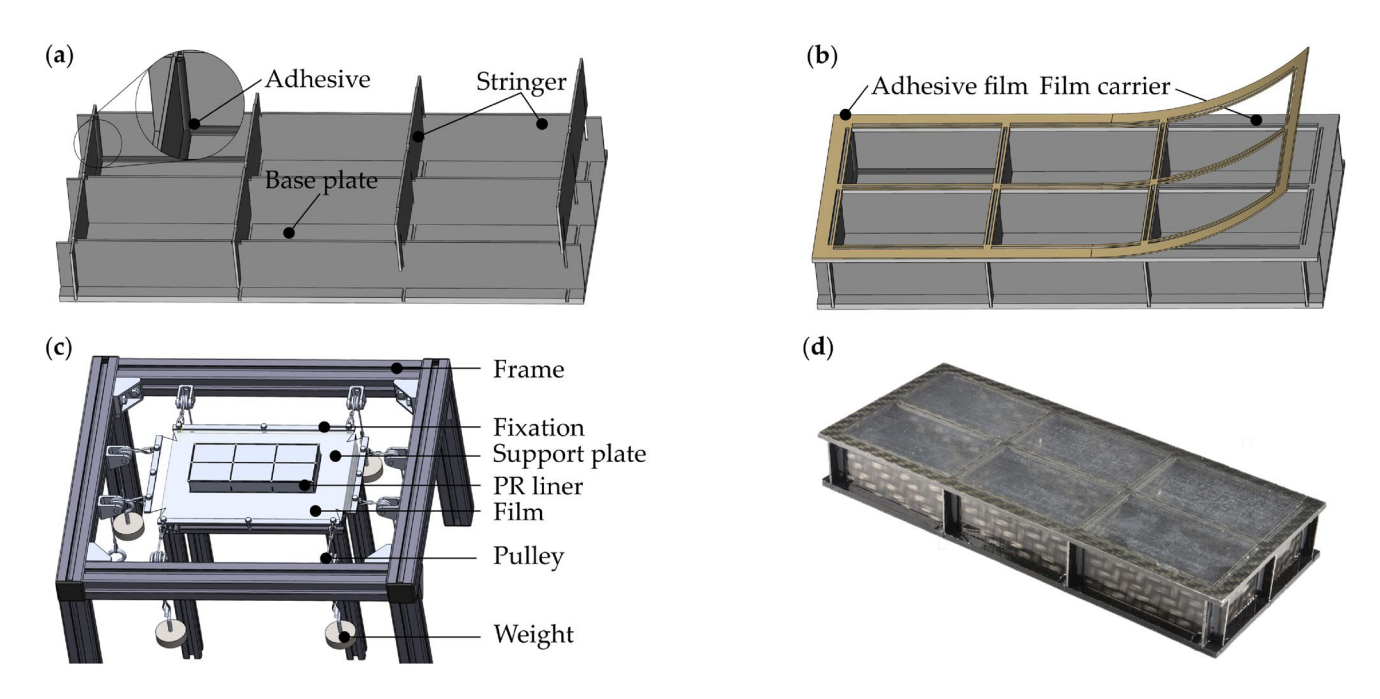


Fig. 6 Assembly process of the planar PR liner sample

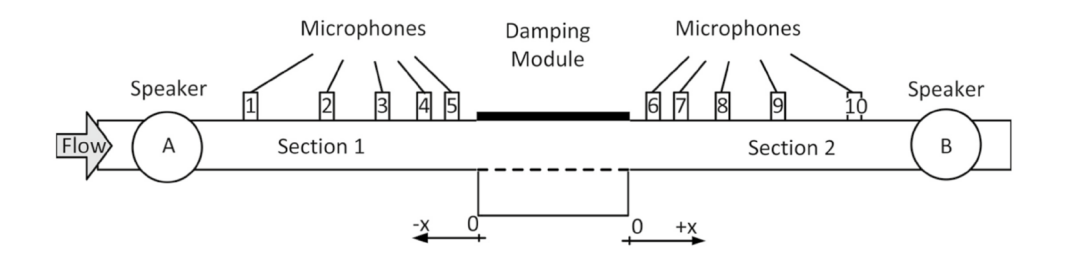


Fig. 7 Schematic view of the DUCT-R test rig

investigations [19–22]. One of the investigated PR liner prototypes is shown in Fig. 8.

5.2 Numerical setup

In addition to the measurements, numerical investigations are conducted on the plate resonator liner. Therefore, the commercial software Actran 2023.2 was used, which facilitates finite element simulations for acoustic applications. The model and the mesh are created using the free software Gmsh and are subsequently imported into Actran. To calculate the scattering coefficients of the PR liner model, a direct frequency response (DFR) is conducted using the FEM-software. Corresponding to the semi-analytical model, only plane incident waves are considered.





Fig. 8 Picture of the PR liner prototype without pre-tension

The considered model is created according to the PR liner prototype in Fig. 8. The material and geometrical parameters correspond to those in Tab. 2 and Tab. 3. The dimensions of the duct with a cross-section of 6cm by 8cm are the same as those of the test rig used in the experiments (see 5.1). The air mesh is discretized into six elements per smallest wavelength, resulting in an element size of 0.02m, for the highest frequency of 2000Hz. However, due to the necessity of considering different sound velocities for airborne and structure-borne sound, the plate mesh must be resolved at a finer scale than those of the duct and the cavities. Thus, the meshes of the TPU plates are modelled with eight elements per smallest wavelength, resulting in an element size of 0.7mm. To prevent unnecessary refinement of the air mesh, the meshes of the duct, plate and cavities are modelled separately. This approach enables the refinement of the plate mesh without resulting in a finer mesh for the fluid above and below it. After the import of the model into Actran, the meshes are then coupled using so-called coupling surfaces. This procedure facilitates a reduction in the number of nodes without compromising the accuracy of the simulations. The used mesh can be seen in Fig. 9. Due to the high density of nodes, the mesh of the TPU plates appears as an almost closed surface. The boundary conditions of the plates are defined as simply supported according to the semi-analytical approach. And as in the experimental setup, the ends of the duct are defined as non-reflecting.

5.3 Results

In this section, the results of the measurements are shown. First, the measured scattering coefficients of the PR liner with and without pre-tension are compared. Afterwards, the measurement results under grazing flow conditions are compared to the semi-analytical model. In the following, the scattering coefficients are considered to investigate not only the overall transmission loss, but also whether this is primarily caused by reflection or dissipation effects.

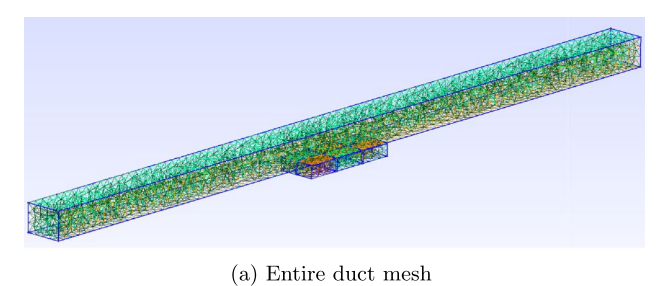
Pre-Tension The measured scattering coefficients of the two PR liner samples are shown in Fig. 10 for M = 0.0. The superscript + denotes downstream and the - denotes upstream sound propagation. Since these results were measured without grazing flow, the respective curves lie exactly on top of each other. First of all, considering the transmission (see Fig. 10a), it is noticeable that the target frequency of 650Hz could not be reached exactly. Instead the damping maximum is around 600Hz. It is remarkable that the transmission curves exhibit almost the same behaviour. Merely, the PR liner without pre-tension shows a bit more broadband attenuation above 650Hz. The measured reflection coefficient is exactly the same for both samples and is comparatively low, see Fig. 10b. The dissipation coefficient shows a different behaviour, due to a high value at the peak and is comparatively broadband, see Fig. 10c. Here again, the dissipation between 650Hz and 800Hz is a bit higher for the PR liner without pre-tension.

In general, it can be assumed that a difference in the pre-tension level leads to a shift of the attenuation peak in frequency. As this could not be observed here, it can be assumed that pre-tension has been reduced due to relaxation processes. Therefore, the minor discrepancies in the curves can be attributed to variations in the manufacturing process.

Flow Before the measurement results under grazing flow conditions are considered, the measurements without pretension and without grazing flow are first evaluated and compared with the semi-analytical model and with the results of the finite element simulations as shown in Fig. 11. Considering the transmission coefficient the frequency shift between measurement and model becomes clear, see Fig. 11a. However, the fact that an even lower frequency could be achieved with the low cavity height of 25mm can be seen as a positive deviation. Additionally, the measured peak is more broadband than the model predicts. This is also a positive deviation and could be due to interactions between the chambers that the model cannot take into account, as the split into several chambers perpendicular to the direction of sound incidence cannot be considered.

The comparison of measurement and semi-analytical model with the results of the FEM shows that in a way the FEM covers both. The falling branch overlaps better with the measurement and the rising branch with the semi-analytical model. Thus, the FEM shows a broadband behaviour that corresponds more to the measurement results than to the semi-analytical model. However, the frequency of the damping maximum, where the transmission is lowest, matches the semi-analytical model somewhat better. The discrepancies between the finite element method (FEM) and the model may be attributed to the FEM's ability to resolve the subdivision of chambers perpendicular to the direction of sound incidence, a capability that the semi-analytical model lacks. However, there appear to be effects in the measurement that





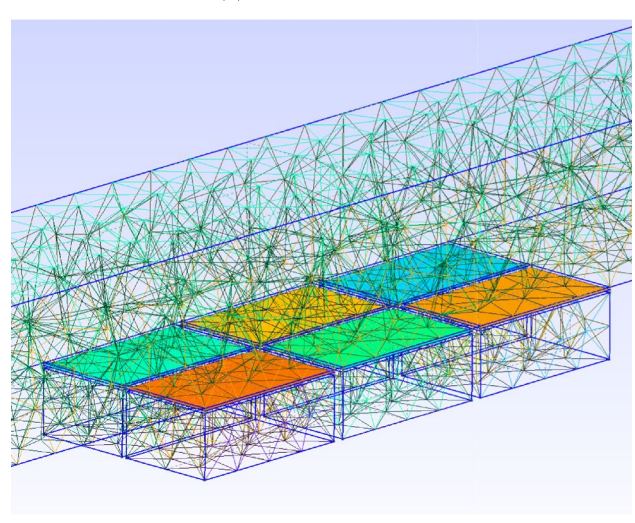


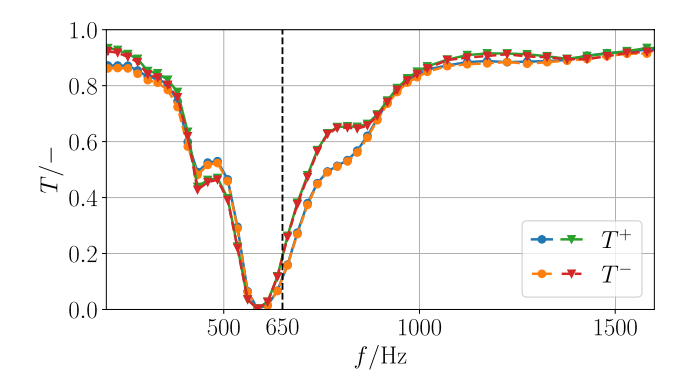
Fig. 9 Finite element mesh of the duct with the PR liner

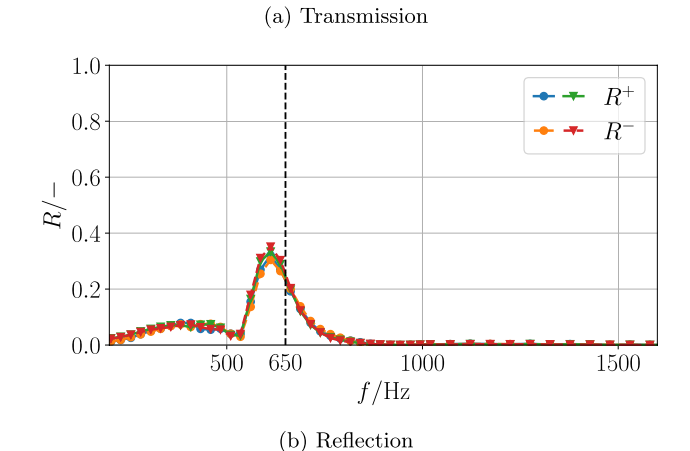
cannot be reproduced by the FEM, which lead to a frequency shift in the measurement.

(b) Detailed mesh of the PR liner

A significant quantitative deviation between all three approaches can be seen for the reflection coefficient, see Fig. 11b. In addition to the frequency shift, the semi-analytical model predicts a stronger reflection than occurs in the measurement data. The reflection coefficient calculated by the FEM lies in between. This means that the FEM shows less reflection than the semi-analytical model, but still more reflection than the measurements, but at a higher frequency, which again fits the model better.

In contrast, the dissipation of the measurement is significantly stronger and more broadband than the semi-analytical model predicts, see Fig. 11c. The finite element method (FEM) results exhibit qualitative agreement with the measurements, surpassing the accuracy of the semi-analytical model. However, the FEM results still overestimate the measured dissipation for certain frequencies. In particular, the consideration of reflection and dissipation implies that there are damping effects that are not considered in the model or in the FEM. The lower dissipation of the semi-analytical model can initially be attributed to overestimated reflection, as the dissipation results from reflection and transmission. However, it is not clear why reflection





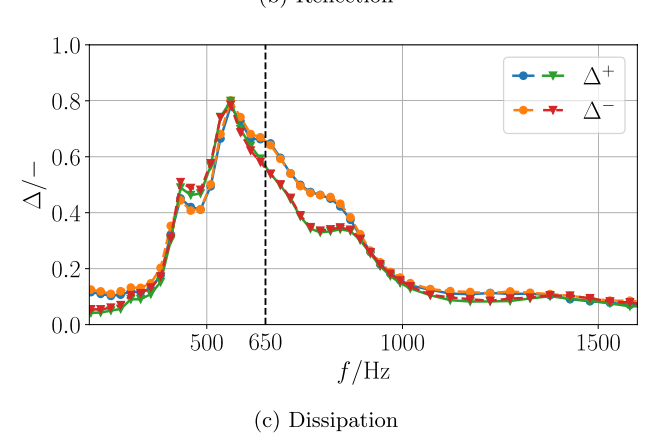


Fig. 10 Comparison of measured scattering coefficients of the PR liner with pre-tension (▼) and without pre-tension (•); solid line: downstream sound propagation, dashed line: upstream sound propagation

is overestimated and dissipation is underestimated. Nevertheless, various mechanisms that could exist in reality but cannot be considered in the model are conceivable. On the one hand, this could be achieved by enhanced interactions between cells, which effectively trap sound waves at perpendicular angles relative to the direction of incidence. This can be indicated by the fact that the dissipation of the FEM fits the measurements better than the semi-analytical model. On the other hand, the glued edges may exert a significant



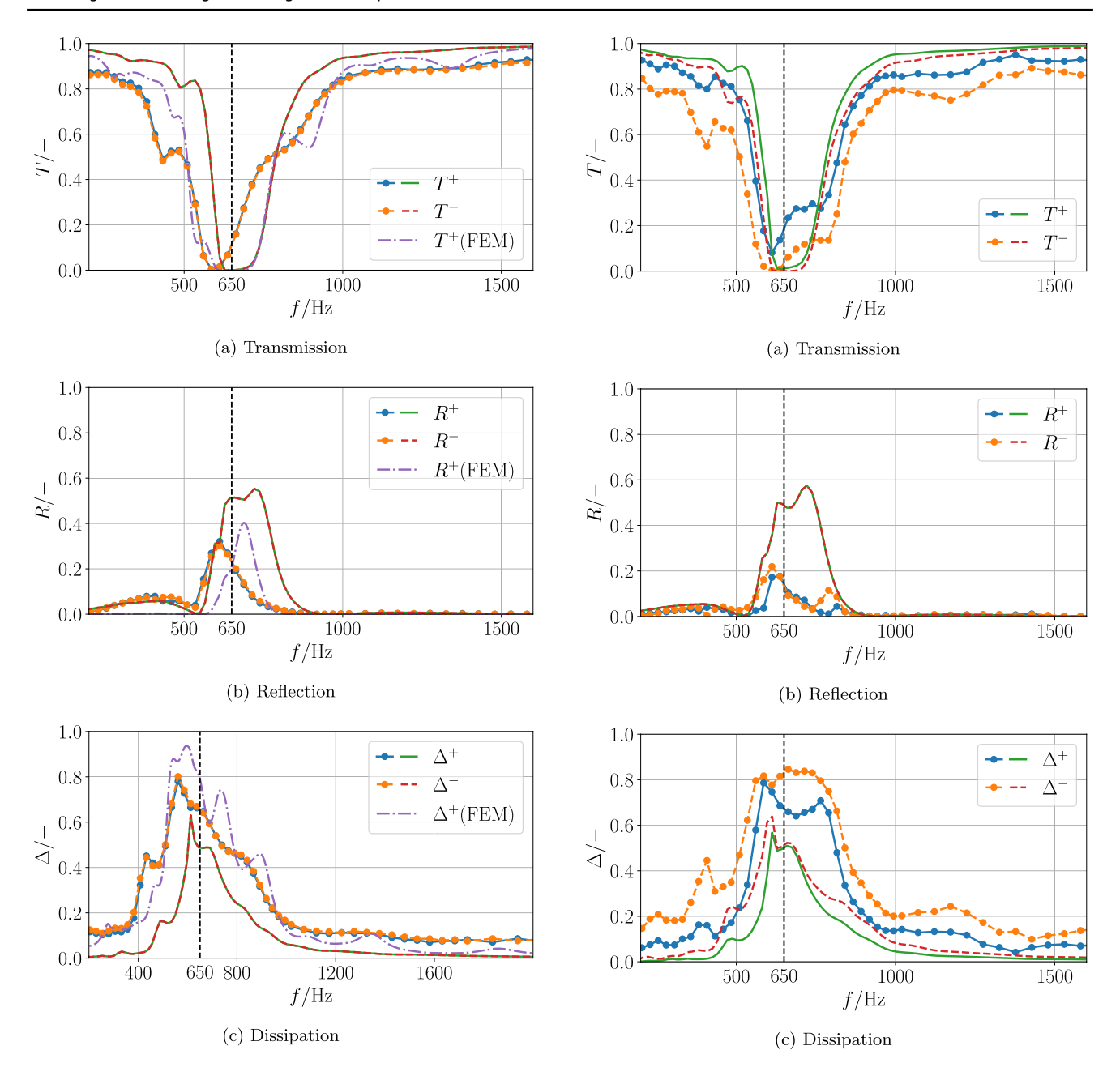


Fig. 11 Comparison of the scattering coefficients of the PR liner sample determined by measurement (\bullet), semi-analytical model and FEM (\neg); M=0.0; solid line: downstream sound propagation, dashed line: upstream sound propagation

Fig. 12 Comparison of measured and calculated scattering coefficients of the PR liner sample; M = 0.2; solid line: downstream sound propagation, dashed line: upstream sound propagation

impact on dissipation, as the gluing process and inherent irregularities can introduce supplementary damping effects at the plate edges. These effects cannot be modelled in the semi-analytical model or in the FEM, and they could also be responsible for the frequency shift.

Finally, the results of the measurements at M = 0.2 are compared with those of the semi-analytical model, see Fig. 12. Considering the transmission coefficient it can

be seen that for upstream sound propagation the dip in the transmission curve is stronger and more broadband than for downstream sound propagation, see Fig. 12a. This means that less sound is transmitted upstream than downstream. Similar effects can also be observed for the semi-analytical model. However, here the difference between upstream and downstream sound propagation is significantly smaller. It is remarkable that the reflection coefficient of the semi-analytical model shows no difference



between upstream and downstream, see Fig. 12b. And a similar trend can be seen for the measurement results as well, even if slight deviations are recognisable here, which could also correspond to usual measurement uncertainties. Due to the grazing flow, the reflected component becomes even smaller. Whereby, the model still significantly overestimates the reflection coefficient. In addition to the previously mentioned factors contributing to the deviation between the measured reflection and the calculated reflection by the semi-analytical model, interactions between the plates and the flow may also be a significant consideration. Such interactions would not be accounted for by the semi-analytical model's assumption of a superimposed base flow. The dissipation coefficient shows a similar behaviour to the transmission coefficient, see Fig. 12c. Upstream sound propagation along the liner leads to a significantly higher and more broadband dissipation, due to the fact that the sound interacts with the liner over a longer period of time. Again, the model shows a similar trend, although the quantitative differences are less pronounced.

Finally, it is particularly noteworthy that the measurement results are shifted to higher frequencies due to the grazing flow. This leads to a better agreement with the model and the target frequency of 650Hz is better achieved. Therefore, the semi-analytical model can be successfully used to design a PR liner for a target frequency under grazing flow conditions. Even though the transmission coefficient could be more broadband, the objective of low-frequency attenuation was achieved with a very low construction height of only 25mm.

The primary objective of this evaluation is to investigate the feasibility of designing a PR liner using a semi-analytical model. However, the question also arises as to how the PR liner compares to other liner technologies. The results presented here can only be directly compared to other studies to a limited extent due to significant variations in underlying conditions. Despite the challenges, an effort will be made to categorize them. In comparison to various single and multidegree-of-freedom liners based on the Helmholtz resonator concept, which were examined in [23], it is evident that the PR liner in this design does not exhibit a broadband effect. In contrast, the PR liner achieves maximum attenuation at frequencies significantly lower than those of these liners, despite having a comparable or even lower overall height, thereby demonstrating clear advantages for attenuating lowfrequency tonal noise. In comparison to a multi-perforatedpanel absorber, as investigated in [24], the PR liner exhibits also slight weaknesses in its broadband attenuation, but also achieves low frequency absorption at significantly lower overall heights. In conclusion, the PR liner concept can achieve low-frequency damping with a relatively low overall height, offering a significant advantage in applications

where engine nacelles are becoming increasingly large and space is limited.

6 Conclusion

This study shows that significant progress was made in the investigation of plate resonators as potential jet engine liners. The semi-analytical modelling has significantly improved the understanding of the operating principle of plate resonators, enabling targeted design and optimisation. This was demonstrated in this study using a flat PR liner prototype. Extensive parameter studies contributed to the understanding of working mechanisms and could be used to select a suitable plate material, which has been analysed for its properties. After designing, a prototype was manufactured in lightweight construction according to engine-specific requirements. The result is a flat PR liner, which achieves the goal of low-frequency attenuation while using low construction height. This was confirmed by measurements in the acoustic test rig under grazing flow conditions. Thus, it can be concluded that the presented PR liner concept is very promising for liner technologies in future jet engines. Furthermore, the transfer of this concept to an engine nacelle was investigated as part of a feasibility study [13].

Finally, it can be concluded that the results have brought the PR liner concept to a very advanced stage providing a solid base for further steps towards technology maturity.

Acknowledgements This work was funded within the framework of the LuFo VI-1 project "FLIER" (Flexible wall structures for acoustic Liners, contract number 20E1915B) by the Federal Ministry for Economic Affairs and Climate Action based on a decision of the German Bundestag, which is gratefully acknowledged. The fruitful collaboration within the consortium (TU Berlin, TU Dresden, BTU Cottbus-Senftenberg) and the external participants Fraunhofer IAP Schwarzheide, Fraunhofer PYCO Wildau, RRD and DLR have made the project's success possible.

A special thanks goes to Felix Schwäricke, whose work has greatly enriched the project.

Author contributions V.R. designed and conducted the semi-analytical calculations, parameter studies and experiments and prepared the manuscript. M.N. designed and manufactured the PR liner prototype. J.G. helped in the design and conduction of the acoustic experiments. F.K. helped in the design and conduction of the acoustic experiments. S.J. helped in the design and conduction of parameter studies and experiments. All authors discussed the results and commented on the manuscript at all stages.

Funding Open Access funding enabled and organized by Projekt DEAL.

Data availability Data sets generated during the current study are available from the corresponding author on reasonable request.

Declarations

Conflict of interest The authors have no Conflict of interest to declare that are relevant to the content of this article.



Open Access This article is licensed under a Creative Commons Attribution 4.0 International License, which permits use, sharing, adaptation, distribution and reproduction in any medium or format, as long as you give appropriate credit to the original author(s) and the source, provide a link to the Creative Commons licence, and indicate if changes were made. The images or other third party material in this article are included in the article's Creative Commons licence, unless indicated otherwise in a credit line to the material. If material is not included in the article's Creative Commons licence and your intended use is not permitted by statutory regulation or exceeds the permitted use, you will need to obtain permission directly from the copyright holder. To view a copy of this licence, visit http://creativecommons.org/licenses/by/4.0/.

References

- Strutt, J.W., Spottiswoode, W.: V. On the theory of resonance. Philosophical Trans. Royal Soc. London 161, 77–118 (1871). https://doi.org/10.1098/rstl.1871.0006
- Leylekian, L., Covrig, A., Maximova, A.: Aviation noise impact management: technologies, regulations, and societal well-being in Europe. Springer, Cham (2022)
- Huang, L.: Broadband sound reflection by plates covering sidebranch cavities in a duct. J. Acoustical Soc. Am. 119(5), 2628– 2638 (2006). https://doi.org/10.1121/1.2186431
- Liu, G., Zhao, X., Zhang, W., Li, S.: Study on plate silencer with general boundary conditions. J. Sound Vib. 333(20), 4881–4896 (2014). https://doi.org/10.1016/j.jsv.2014.05.019
- Kisler, R., Sarradj, E.: Plate silencers for broadband low frequency sound attenuation. Acta Acustica United Acustica 104(3), 521– 527 (2018). https://doi.org/10.3813/AAA.919194
- Fuchs, H.V.: Applied acoustics: concepts, absorbers, and silencers for acoustical comfort and noise control: alternative solutions innovative tools - practical examples. Springer, Berlin, Heidelberg (2013)
- Callaway, V.E., Goralski, L.S.: Sound energy absorbing apparatus. US patent 3,439,774, 1969. US Patent 3,439,774
- Wang, C., Huang, L.: Analysis of absorption and reflection mechanisms in a three-dimensional plate silencer. J. Sound Vib. 313(3-5), 510-524 (2008). https://doi.org/10.1016/j.jsv.2007.12. 027
- Huang, L., Choy, Y.S.: Vibroacoustics of three-dimensional drum silencer. J. Acoustical Soc. Am. 118(4), 2313–2320 (2005). https://doi.org/10.1121/1.2010353
- Wang, C., Cheng, L., Huang, L.: Realization of a broadband low-frequency plate silencer using sandwich plates. J. Sound Vib. 318(4–5), 792–808 (2008). https://doi.org/10.1016/j.jsv.2008. 04.054
- Wang, C., Han, J., Huang, L.: Optimization of a clamped plate silencer. J. Acoustical Soc. Am. 121(2), 949–960 (2007). https:// doi.org/10.1121/1.2427126
- 12. Radmann, V., Kohlenberg, F., Sarradj, E.: Modeling of a 3D plate resonator liner and comparison to numerical and experimental

- investigations. In: AIAA AVIATION 2023 forum. American institute of aeronautics and astronautics, San Diego, CA and Online (2023). https://doi.org/10.2514/6.2023-3639
- Neubauer, M., Genßler, J., Radmann, V., Kohlenberg, F., Pohl, M., Böhme, K., Knobloch, K., Sarradj, E., Höschler, K., Modler, N., Enghardt, L.: Experimental and numerical investigation of novel acoustic liners and their design for aero-engine applications. Aerospace 10(1), 5 (2023). https://doi.org/10.3390/aerospace10010005
- Neubauer, M., Schwaericke, F., Radmann, V., Sarradj, E., Modler, N., Dannemann, M.: Material selection process for acoustic and vibration applications using the example of a plate resonator. Materials 15(8), 2935 (2022). https://doi.org/10.3390/ma150 82935
- Wang, C.: Development of a broadband silencer in flow duct. PhD thesis. The Hongkong Polytechnic University, Hongkong (2007)
- Inman, D.J.: Engineering Vibration, 3rd edn. Pearson eduction Inc, Upper Saddle River, New Jersey (2008)
- Radmann, V., Schwäricke, F., Jekosch, S., Sarradj, E.: Acouplasi v24.04. Zenodo (2024). https://doi.org/10.5281/zenodo.10996772
- Ashby, M.F.: Overview no. 80. Acta Metallurgica 37(5), 1273–1293 (1989). https://doi.org/10.1016/0001-6160(89)90158-2
- Knobloch, K., Enghardt, L., Bake, F.: Investigation of flexible walls for acoustic liners. In: 25th AIAA/CEAS Aeroacoustics Conference. American institute of aeronautics and astronautics, Delft, The Netherlands (2019). https://doi.org/10.2514/6. 2019-2565
- Lahiri, C., Enghardt, L., Bake, F., Sadig, S., Gerendás, M.: Establishment of a high quality database for the acoustic modeling of perforated liners. J. Eng. Gas Turbines Power (2011). https://doi.org/10.1115/1.4002891
- Busse-Gerstengarbe, S., Bake, F., Enghardt, L., Jones, M.G.: Comparative study of impedance eduction methods, part 1: DLR tests and methodology. In: 19th AIAA/CEAS aeroacoustics conference. American institute of aeronautics and astronautics, Berlin, Germany (2013). https://doi.org/10.2514/6.2013-2124
- Schulz, A.: Die akustischen Randbedingungen perforierter Wandauskleidungen in Strömungskanälen Physikalische Modelle und Eduktion. PhD thesis, Technische Universität Berlin (2019). https://doi.org/10.14279/DEPOSITONCE-7943
- Palani, S., Murray, P., McAlpine, A., Knepper, K., Richter, C.: Experimental and numerical assessment of novel acoustic liners for aero-engine applications. In: 28th AIAA/CEAS aeroacoustics 2022 conference. American institute of aeronautics and astronautics, Southampton, UK (2022). https://doi.org/10.2514/6.2022-2900
- Li, Y., Choy, Y.S.: Acoustic behaviour of micro-perforated panel backed by shallow cavity under fully developed grazing flow. J. Sound Vib. (2024). https://doi.org/10.1016/j.jsv.2023.117985

Publisher's Note Springer Nature remains neutral with regard to jurisdictional claims in published maps and institutional affiliations.

